

Matthew J. Nielsen*, A. S. Jones, J. M. Forsythe, and T. H. Vonder Haar

DoD Center for Geosciences / Atmospheric Research (CG/AR)
Cooperative Institute for Research in the Atmosphere (CIRA)
Colorado State University
Fort Collins, CO

1. INTRODUCTION

Water vapor is a fundamentally important variable in the atmosphere for making accurate forecasts. Its global distribution is a challenge to determine and can change rapidly. Several methods are currently employed to determine its spatial and temporal variability. Such methods include the use of Radiosondes, radars, satellite borne infrared sounders, Global Positioning System (GPS) measurements from both space based and ground based receivers, and microwave radiometers.

Microwave remote sensing techniques were first developed and used in the 1930's to measure energy from non-Earth sources. Over the last thirty years, the focus has come back to measuring radiation from our own planet. Today we use satellite borne radiometers to retrieve temperature and water vapor data over the Earth. One such instrument being employed is the Advanced Microwave Sounding Unit – B (AMSU-B) aboard the NOAA-15 satellite. AMSU-B is a five-channel microwave radiometer with three channels at 183.3 GHz and two additional channels centered at 89 and 150 GHz. Ninety Earth views are made every 2.667 seconds with viewing angles from -48.95° to $+48.95^\circ$ with a sampling distance of about 1.10° . The radiometer receives around 95% of the total power from the antenna's mainbeam, which is typically pointed at an Earth scene. The remaining 5% or so of the energy comes from Earth, cold space, and satellite platform sidelobes. The exact mainbeam efficiencies are given by Table 1.

Removing these sidelobes is an essential task for retrieving true temperature and moisture data. Energy from the sidelobes introduces a bias in the retrieved brightness temperature that introduces a bias into the retrieved water vapor measurements.

Removing this bias will improve the accuracy of the temperature and water vapor retrievals, which can then be used in data assimilation schemes, climate models, as well as in data analysis.

| Main Beam Efficiencies | | | | | | |
|------------------------|------------|-------|------|------|------|---------------|
| Channel | Freq.(GHz) | Pixel | PFM | FM2 | FM3 | Specification |
| 16 | 87.9 | 45 | 94.4 | 94.4 | 94.9 | >95.0 |
| 17 | 148.8 | 45 | 95.1 | 94.9 | 94.9 | >95.0 |
| 19 | 186.3 | 45 | 96.9 | 96.2 | 96.5 | >95.0 |

Table 1: Measured AMSU-B mainbeam efficiencies

2. METHODOLOGY

The mainbeam width for AMSU-B is about $1.10^\circ +$ or $- 0.2^\circ$ depending on which channel is being used. Anywhere from 94.4% to 96.9% of the total energy from the radiometer is received in this very small angle. The remaining 3.1%-5.4% of the energy comes from sidelobe sources. These sidelobes are distributed among the remaining three scene categories: 1) Earth outside of the mainbeam, 2) cold space, 3) and the satellite platform. If it is assumed that the satellite platform does not absorb a significant amount of radiation, then that source can be neglected. After this assumption is made, then the cold space and Earth sidelobes can be determined by dividing the remaining energy from the radiometer between the two scenes. This division can be determined by a straightforward geometrical argument. By determining the solid angle that the Earth subtends as it moves through all 90 scan angles, an Earth fraction can be calculated. This Earth fraction can then be used to determine the amount of energy that should be distributed to the Earth sidelobe. The remaining energy is allocated to the cold space sidelobe. The antenna temperature is then

* Corresponding author address: Matthew J. Nielsen, Colorado State University / Cooperative Institute for Research in the Atmosphere (CIRA), Fort Collins, CO 80523-1375; e-mail: nielsen@cira.colostate.edu.

a sum of the mainbeam retrieved temperature and the sidelobes:

$$T_A(\theta) = [E_e(\theta)T_E + E_c(\theta)T_C + E_{es}(\theta)T_{es}] \quad (1)$$

where $T_A(\theta)$ is the antenna temperature measured as a function of scan angle θ , $E_e(\theta)$ is the mainbeam efficiency, T_E is the true brightness temperature of Earth, $E_c(\theta)$ is the cold space sidelobe efficiency, T_C is the cold space temperature (assumed to be a constant of 2.73K), $E_{es}(\theta)$ is the Earth sidelobe efficiency, and T_{es} is the Earth sidelobe brightness temperature.

From Eq. (1), the brightness temperature can be solved as a function of antenna temperature, which is in turn a function of the scan angle.

$$T_E = [T_A(\theta) - E_c(\theta)T_C] / [E_e(\theta) + E_{es}(\theta)] \quad (2)$$

This approach contains some underlying assumptions. The most important assumption deals with the uniform Earth brightness temperature. By imposing a restriction that holds the Earth brightness temperature fixed over both the mainbeam swath and the sidelobes, a very simple and crude antenna pattern correction can be calculated. Unfortunately the brightness temperature of the Earth can vary dramatically over very sharp boundaries. Coastlines in particular are sensitive to this assumption, due to the dramatic emissivity differences between ocean and dry land. Another related scenario can be seen with the ocean and ice interface found in the polar regions. Both again have varying emissivities, and therefore have a large contrast in brightness temperatures.

Other approaches have been adopted to perform antenna pattern corrections for AMSU-A as described by Mo (1999). That approach uses the far-field patterns along with a slightly adjusted satellite platform to determine the antenna temperature. The Earth sidelobe contributions are dealt with differently, however, due to the fact that Mo includes these in his brightness temperature assumptions. Therefore, in the Mo (1999) approach, the antenna temperature (3) has three fundamental terms: the mainbeam contribution, the sidelobe contribution, and the satellite platform contribution.

$$T_A(\beta) = (1/N\eta) [f_e(\beta)T_E + f_c(\beta)T_C + \eta f_{sat}(\beta)T_{SAT}] \quad (3)$$

In order to differentiate the far-field contributions from the near-field contributions, a scale factor η is introduced to the satellite platform term. This scale factor varies for individual channels and is the ratio of a simulated near-field effect on antenna efficiency at the cold calibration position CC1 to the individual satellite efficiencies given by each corresponding channel. The renormalization factor $(1/N\eta)$ is necessary due to the introduction of the scale factor, and is simply the sum of the mainbeam, cold space, and normalized satellite antenna efficiencies. Mo makes supporting arguments that the contribution from the satellite platform is quite small compared to other error and bias contributions. The typical antenna pattern corrections were between 0.5K and 2.5K for each channel.

Another approach to antenna pattern corrections has been developed by the Jet Propulsion Laboratory in Pasadena, California. Their approach is similarly geometric in nature, and determines the antenna temperature by dividing the received radiation among the mainbeam, space sidelobes, and the Earth sidelobes. With an assumed brightness temperature of 250 K, a simulated satellite orbit identical to that of AMSU-B was used to calculate simulated antenna temperatures. At nadir, a difference of 5.1 K is noted. At a scan angle of 50° (nearly that of the maximum scan angle of AMSU-B) the difference grows to 7.5K.

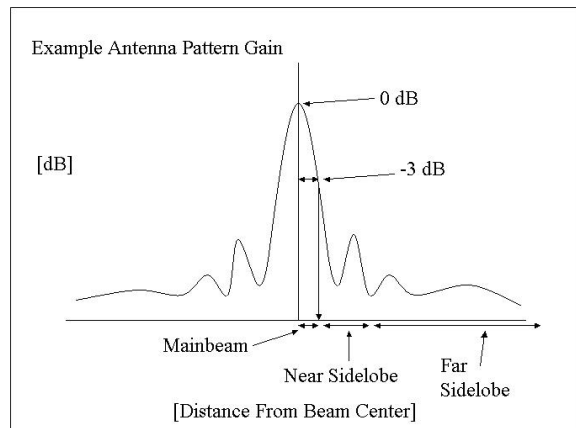


Figure 1: An Example of an Antenna Pattern Gain

3. RESULTS AND CONCLUSIONS

Two separate simulations were conducted in order to quantify the effect of antenna pattern

corrections as a function of scan angle and as a function of brightness temperature. These intercomparison results will be presented at the 13th Satellite Meteorology and Oceanography Conference in Norfolk, Virginia. Preliminary work shows that antenna pattern correction values are linear with temperature dependence, and non-linear with scan angle dependence. Since temperature is a linear function in Eq. 2, we expect to see this linearity in the antenna pattern correction. Due to the geometric nature of the Earth fraction, the antenna efficiencies vary non-linearly.

The purpose of performing this antenna pattern correction was to quantify the bias introduced by sidelobe contamination. Once this bias has been determined, it is then necessary to consider whether or not this bias is significant. After running the simulation at various scan angles and at differing brightness temperatures, biases of 2-3K or higher were observed. These biases constitute relative errors in brightness temperature of up to 5% or higher in some cases. Thus these biases have been shown to have a significant impact on water vapor retrievals.

Antenna pattern corrections are an essential part of microwave remote sensing data analysis. Removing errors and biases from retrieved data assures that information that is passed to data assimilation systems and forecast models is accurate and useful. Currently some data analysis systems lack a proper procedure for far sidelobe removal, making the information obtained by these procedures questionable. Adopting an antenna pattern correction will assure that far sidelobe

contamination has been taken into account, thereby increasing the accuracy and confidence of temperature and water vapor observations globally.

REFERENCES

- Goodrum, G., K.B. Kidwell, and W. Winston, Eds., 1999: NOAA KLM User's Guide. National Oceanic and Atmospheric Administration
- Hewison, T.J., and R. Saunders, 1996: Measurements of the AMSU-B antenna pattern. *IEEE Trans. Geosci. Remote Sens.*, 31, 405-412
- Jet Propulsion Laboratory, 2000: AIRS Project: Algorithm Theoretical Basis Document: Microwave Instruments, Version 2.1, pp41-46
- Mo, T., 1999: AMSU-A antenna pattern corrections. *IEEE Trans. Geosci. Remote Sens.*, 37, 103-112
- Saunders, R.W., Hewison, T.J., Atkinson, N.C., and Stringer, S.J. "The radiometric characterization of AMSU-B," *IEEE Trans. Microwave Theory Tech.*, vol. 43, pp. 760-771, May 1995

ACKNOWLEDGMENTS

This work was supported in part by CloudSAT at NASA-Goddard under contract agreement NAS5-99237, the DoD Center for Geosciences/Atmospheric Research at Colorado State University under the Cooperative Agreements DAAD19-01-2-0018 with the Army Research Laboratory, and by the Joint Center for Satellite Data Assimilation (JCSDA) program via NOAA grant NA17RJ1228#15 under CIRA's cooperative agreement with NOAA.